AD-A071 595 PENNSYLVANIA STATE UNIV UNIVERSITY PARK DEPT OF MATE--ETC F/G 11/6
EFFECT OF HELIUM-, IRON-, AND PLATINUM- ION IMPLANTATION ON THE--ETC(U)
JUL 79 M ZAMANZADEH, A ALLAM, H W PICKERING N00014-75-C-0264

UNCLASSIFIED TR-10 NL

END
DATE FILMED
8-79
DDC

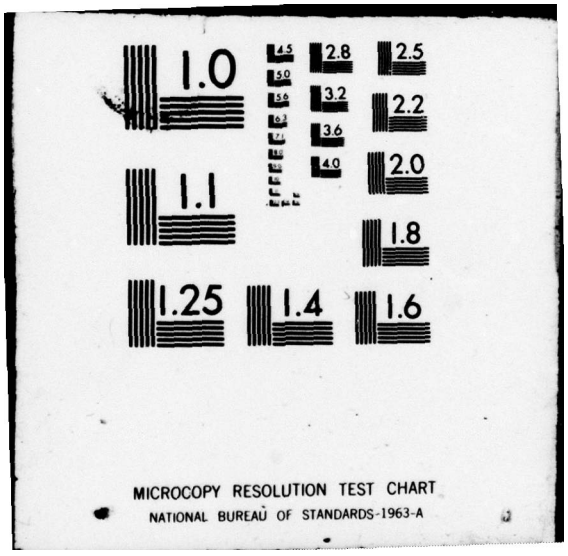
1.0
1.1
1.25
1.4
1.6
1.8
2.0
2.2
2.5
2.8
3.2
3.6
4.0
4.5
5.0
5.6
MICROCOPY RESOLUTION TEST CHART
NATIONAL BUREAU OF STANDARDS-1963-A

LEVEL II

12

THE COLLEGE OF EARTH AND MINERAL SCIENCES

DEPARTMENT OF MATERIALS SCIENCE AND ENGINEERING

METALLURGY SECTION

The Pennsylvania State University
University Park, Pennsylvania 16802

TECHNICAL REPORT NO. 10

to

OFFICE OF NAVAL RESEARCH

Contract No. N000-14-75-C-0264

EFFECT OF HELIUM-, IRON-, AND PLATINUM- ION IMPLANTATION ON THE PERMEATION OF HYDROGEN THROUGH IRON MEMBRANES

BY

M. ZAMANZADEH, A. ALLAM, H. W. PICKERING

AND

G. K. HUBLER
NAVAL RESEARCH LABORATORY
WASHINGTON, D.C. 20375

THE PENNSYLVANIA STATE UNIVERSITY

UNIVERSITY PARK, PENNSYLVANIA

THE PENNSYLVANIA STATE UNIVERSITY

COLLEGE OF EARTH AND MINERAL SCIENCES

UNDERGRADUATE PROGRAMS OF STUDY:

Ceramic Science, Earth Sciences, Geography, Geological Sciences, Metallurgy, Meteorology, Mineral Economics, Mining, Petroleum and Natural Gas, Polymer Science

GRADUATE PROGRAMS AND FIELDS OF RESEARCH:

Ceramic Science, Fuel Science, Geochemistry, Geography, Geology, Geophysics, Metallurgy, Meteorology, Mineral Economics, Mineral Processing, Mineralogy and Petrology, Mining Engineering, Petroleum and Natural Gas Engineering

INTERDISCIPLINARY GRADUATE PROGRAMS:

Earth Sciences, Environmental Pollution Control, Mineral Engineering Management, Solid State Science

ASSOCIATE DEGREE PROGRAMS:

Materials Technology
Mining Technology

INTERDISCIPLINARY RESEARCH SECTIONS:

Coal Research, Mass Spectrometry, Mine Drainage, Mineral Conservation, Ore Deposits

ANALYTICAL AND STRUCTURE STUDIES:

Classical Chemical Analysis of metals and silicate and carbonate rocks, X-Ray Crystallography, Electron Microscopy and Diffraction, Electron Microprobe Analysis, Atomic Absorption Analysis, Spectrochemical Analysis

SECURITY CLASSIFICATION OF THIS PAGE (When Data Entered)

REPORT DOCUMENTATION PAGE

READ INSTRUCTIONS BEFORE COMPLETING FORM

1. REPORT NUMBER: Technical Report No. 10
2. GOVT ACCESSION NO.:
3. RECIPIENT'S CATALOG NUMBER:

4. TITLE (and Subtitle): Effect of Helium-, Iron-, and Platinum- Ion Implantation on the Permeation of Hydrogen through Iron Membranes

5. TYPE OF REPORT & PERIOD COVERED: Technical Progress Report

6. PERFORMING ORG. REPORT NUMBER:

7. AUTHOR(s): M. Zamanzadeh, A. Allam, H. W. Pickering and G. K. Hubler*

8. CONTRACT OR GRANT NUMBER(s): N000-14-75-C-0264

9. PERFORMING ORGANIZATION NAME AND ADDRESS:
Department of Materials Science & Engineering
Metallurgy Section
The Pennsylvania State University
University Park, PA 16802

10. PROGRAM ELEMENT, PROJECT, TASK AREA & WORK UNIT NUMBERS:

11. CONTROLLING OFFICE NAME AND ADDRESS:
Metallurgy Branch
Office of Naval Research
Arlington, VA 22217

12. REPORT DATE: July 1979

13. NUMBER OF PAGES: 24

14. MONITORING AGENCY NAME & ADDRESS (if different from Controlling Office):

15. SECURITY CLASS. (of this report): Unclassified

15a. DECLASSIFICATION/DOWNGRADING SCHEDULE:

16. DISTRIBUTION STATEMENT (of this Report)

Distribution of this document is unlimited

DISTRIBUTION STATEMENT A
Approved for public release;
Distribution Unlimited

17. DISTRIBUTION STATEMENT (of the abstract entered in Block 20, if different from Report)

18. SUPPLEMENTARY NOTES

*Naval Research Laboratory
Washington, D. C. 20375

19. KEY WORDS (Continue on reverse side if necessary and identify by block number)

Hydrogen permeation, catalytic mechanism, ion implantation, hydrogen evolution, selective dissolution

20. ABSTRACT (Continue on reverse side if necessary and identify by block number)

See abstract

S/C

DD FORM 1 JAN 73 1473 EDITION OF 1 NOV 65 IS OBSOLETE
S/N 0102-LF-014-6601

404352

SECURITY CLASSIFICATION OF THIS PAGE (When Data Entered)

(6) EFFECT OF HELIUM-, IRON-, AND PLATINUM- ION IMPLANTATION ON THE PERMEATION OF HYDROGEN THROUGH IRON MEMBRANES.

(10) M./Zamanzadeh, A./Allam, and H. W./Pickering G.K./Hubler
Metallurgy Section
Department of Materials Science and Engineering
The Pennsylvania State University
University Park, Pennsylvania 16802

(11) Jul 79

(12) 28 p.

and

(14) TR-10

G. K. Hubler
Naval Research Laboratory
Washington, D. C. 20375

(15) N00014-75-C-0264

Accession For	
NTIS GRA&I	X
DDC TAB	
Unannounced	
Justification	
By	
Distribution/	
Availability Codes	
Dist	Avail and/or special
A	

(9) Technical progress rept.,

404 352 xlt

ABSTRACT

A preliminary study was made of the effect of various ions implanted in iron on the absorption of hydrogen by Ferrovac-E iron. Using the permeation technique, it was found that the location of implanted Pt, as modified by selective dissolution of iron from the surface, affects the kinetics of the hydrogen evolution reaction and, hence, of the hydrogen absorption process. The rate of hydrogen absorption decreased with increase in Pt concentration on the surface in both 0.1N NaOH and 0.1N H_2SO_4. A catalytic mechanism is proposed to explain the marked reduction in hydrogen permeation. There are no significant differences in the permeation behavior of unimplanted and helium- or iron-implanted iron membranes in 0.1N NaOH. The experimentally observed Tafel slope, the permeation-charging potential relationship, and the permeation-charging current relationship indicate a coupled discharge-recombination mechanism of hydrogen evolution on He-, Fe- or Pt-implanted iron. At higher cathodic overpotentials in 0.1N NaOH, corresponding to potentials more negative than -1.0V (SHE), another mechanism of hydrogen evolution is indicated.

Selective dissolution of iron from the Pt-implanted Fe surface layer is indicated by Rutherford backscattering analyses to involve diffusion of Pt into the iron ahead of the receding surface.

INTRODUCTION

Hydrogen absorption greatly reduces the mechanical properties of structural alloys. A number of investigators have studied the possibility of reducing hydrogen absorption by coatings (1-4). Besides functioning as barriers to hydrogen entry, coatings may also reduce hydrogen absorption through their effect on the kinetics of the hydrogen evolution reaction and, hence, of the hydrogen absorption process. Chatterjee et al. (4) provided experimental confirmation for the catalytic mechanism of decreasing hydrogen entry into iron. They found that discontinuous electrodeposited coatings of Pt, Ni or Cu on iron are effective in reducing hydrogen entry into the membrane. Ion implantation of metals is another method for altering the surface chemically and, thus, also the mechanism and kinetics of the hydrogen evolution reaction, without affecting bulk physical or mechanical properties.

Ashworth and co-workers (5) were among the first to report the effect of ion implantation on the polarization behavior of iron. They found that there is no significant differences between the polarization behaviors of unimplanted and argon-implanted iron beyond that due to changes in surface roughness associated with the implantation process. Other implanted ions in iron, such as chromium and lead, were shown to influence the polarization behavior (6,7).

This paper reports the results of initial studies directed at evaluating the effect of implanted ions on hydrogen permeation through implanted membranes. No other studies of hydrogen permeation of implanted membranes are known to be reported in the literature. Specifically, the goals of this work are:

1. To determine whether, and to what extent, implanted platinum, helium or iron reduce hydrogen permeation through iron.

2. To evaluate if the nature or proximity to the surface of any of these implanted ions affects the mechanism or kinetics of the hydrogen evolution reaction and, hence, of the hydrogen absorption process.

3. To determine the effects of implantation on the effective hydrogen diffusivity which may be related to trapping characteristics.

The rationale behind choosing Pt for implantation is that Pt is one of the best electrocatalysts for the hydrogen evolution reaction. In order to sort out any effects due to the implantation process, itself, the inert element, He, and the substrate element, Fe, were also chosen for comparison with results obtained for the Pt-implanted iron membranes.

EXPERIMENTAL PROCEDURE

The hydrogen permeation measurements were carried out on Ferrovac-E iron. The Fe membranes were prepared by cold rolling wafers cut from a master ingot to the required thickness (0.365mm). After polishing to 600 grit, they were degreased using benzene and methanol in a soxhlet apparatus, and then annealed for two hours at 1000°C in an argon-filled silica capsule. The latter treatment produced an etched surface. One side of some of these membranes was implanted with Fe^+, He^+ or Pt^+ ions at fluences and energies given in Table 1. The samples were implanted in a vacuum of 1×10^{-6} Torr and were in close proximity to a cold surface at liquid nitrogen temperatures (77°K) which minimized carbon contamination. The temperature of the samples during implantation did not exceed 50°C. The implanted samples were stored in an evacuated desicator. Prior to the permeation runs, the Pt content on the surface of the Pt-implanted membranes was increased by selective dissolution of iron via immersion in 1M H_2SO_4 for 20 seconds. Permeation measurements were also made after subsequent 10-second immersions in 0.1N H_2SO_4. Sulfuric acid is known to selectively remove iron from a Fe-Pt solid solution (8).

Electrolyte solutions were prepared from conductivity water (doubly distilled) prepared by the method of Powers (9) and reagent grade chemicals. Final purification was made by pre-electrolyzing the solutions in an external cell prior to admitting them to the permeation cell.

The technique of Devanathan and Stachurski (10) was used to measure the permeability of hydrogen through a membrane while evolving hydrogen off the implanted surface. In this method, a thin metallic membrane is electrolytically charged with hydrogen on the implanted side while on the other side the hydrogen which has diffused through the membrane is anodically oxidized. The orifice of the cell and, thus, the charging area was 0.785 cm^2. The measured anodic current is a direct measure of the hydrogen flux through the membrane for the conditions at the exit surface, which included a thin palladium coating and an oxidizing potential of .018 V(SHE) using a Hg/HgO reference electrode in 0.1N NaOH. These are the same conditions found previously to be suitable for oxidizing all of the hydrogen arriving at the anodically polarized surface (4). The reported values are the measured values after correction for the residual current which is typically less than 1 $\mu A\ cm^{-2}$. The potential of the charging surface was measured using a Hg/Hg_2SO_4 reference electrode in 0.1N H_2SO_4 and a Hg/HgO reference electrode in 0.1N NaOH. Both chambers of the cell were deaerated by bubbling oxygen-free nitrogen through the solutions. The permeation measurements were performed under conditions of cathodic protection. Details of the cell and circuitry are reported elsewhere (4).

The permeation data were obtained as follows. The Fe- and He-implanted iron membranes were precharged at i_c = 0.10 $mA\ cm^{-2}$ for 45 minutes by which time a quasi-stationary permeation current was established. The Pt-implanted

membranes were similarly precharged at 1 mA cm^{-2} (~15 minutes in 0.1N NaOH and ~7 minutes in 0.1N H_2SO_4). The membranes were then charged galvanostatically in 0.02 mA cm^{-2} steps in 0.1N NaOH or in 0.2 mA cm^{-2} steps in 0.1N H_2SO_4 in descending and then ascending directions. Each charging current was maintained for about 4 minutes by which time a quasi-stationary permeation current was established. This procedure has been found to give constant and reproducible permeation transients dependent only on the charging conditions for a given specimen.

Some of the implanted ion-concentration profiles were measured by means of high resolution Rutherford backscattering of alpha particles with a depth resolution of 4 nm. For this measurement, the surface to be implanted was first polished to a mirror finish with 6 μm diamond paste. Details of this method may be found elsewhere (11,12).

RESULTS

Table 2 shows that the steady-state hydrogen permeation fluxes, i_∞, and electrode potentials at the charging side, E_c, in 0.1N NaOH are the same for implanted Fe membranes and identical membranes implanted with He or Fe ions. The permeation transients prior to steady state were also the same within the experimental error for these membranes; the half-rise time ($t_{1/2}$) was 5.5 ± 1.0 seconds. Typical permeation transients are shown in Figure 1.

The effective diffusivity, calculated using the expression (13,14)

$$D = \frac{0.138\ L^2}{t_{1/2}}$$

where L is the membrane thickness, is $D = 3 \times 10^{-5}$ cm^2 s^{-1}. This value is in good agreement with literature values for well-annealed iron (15) and is

also essentially the value obtained by extrapolation of high temperature diffusion data to room temperature (16). The experimentally observed Tafel slope is -122 ± 5mV. This value is the same as that reported for hydrogen evolution on Fe in 0.1N NaOH (17).

Figure 2 shows distribution profiles of Pt implanted in Fe after different amounts of iron dissolution (Pt enrichment of the surface) in 1M H_2SO_4 at room temperature. After 20 seconds immersion in the acid, the Pt concentration at the surface is significantly higher (~3%) than in the as-implanted case ($\lesssim$0.1%). The area under the profile of the 20-second immersed surface is about equal to the area of the as-implanted profile; this indicates that the Pt content of the iron is essentially unchanged during the first 20 seconds in 1M H_2SO_4. After the next 20-second dissolution period in 1M H_2SO_4, the Pt content is much less and nearly at background levels, which indicates that most of the Pt is lost from the membrane during this second dissolution process, probably as particles which dislodge from the surface. Permeation measurements were mainly done, therefore, after an initial 20-second exposure of the Pt-implanted membranes to 1M H_2SO_4.

Figure 3 shows a linear dependence of the steady-state permeation current density on the square root of the charging current density with the curve passing through the origin for an unimplanted Fe membrane and a Pt-implanted Fe membrane following a 20-second immersion in 1M H_2SO_4. This is taken as an indication of a diffusion controlled hydrogen permeation process (17,18). The permeation transient for this membrane is shown in Figure 1. The hydrogen permeability is less at all charging currents for the Pt-implanted than for the unimplanted iron membranes. Pt implantation which is not modified by iron dissolution was found to have an insignificant effect on the hydrogen

evolution and absorption kinetics.

The electrode potentials for hydrogen evolution on the Pt-implanted (and enriched) membrane are invariably more noble than those on the unimplanted membrane, Figure 4. The Tafel slope is -122 ± 5 mV for both unimplanted and Pt-implanted iron. Permeation-charging potential curves for unimplanted and Pt-implanted Fe membranes are given in Figure 5 for the 0.1N NaOH charging solution. The slopes of these curves of the unimplanted Fe membrane at low overpotentials and of the Pt-implanted Fe membrane at all overpotentials are -255 ± 5 mV. Similar results are obtained for a 0.1N H_2SO_4 charging solution, although a change in slope was not observed for the unimplanted Fe. Table 3 lists the relevant data for the 0.1N H_2SO_4 charging solution.

Both, the measured electrode potential of the Pt-implanted surface and the permeation rate of hydrogen through the Pt-implanted membrane during hydrogen charging are functions of the time of immersion in, and concentration of, sulfuric acid. Figure 6 shows the trends in potential and permeation after additional 10-second periods of selective dissolution of iron in a diluted sulfuric acid. The positive effect of Pt enrichment of the surface is seen to hold for an additional amount of dissolution (40 seconds in 0.1N H_2SO_4 following the original 20 seconds in 1M H_2SO_4) before loss of Pt from the surface is indicated by reversal of the electrochemical parameters.

DISCUSSION

The electrocatalytic activity of a surface for the hydrogen evolution reaction can be estimated from the overpotential required to evolve hydrogen at a given current density - the lower the overpotential or the more noble the electrode potential, the more catalytic the surface. Figure 4 and Table

3 show the cathodic potentials obtained in alkaline- and acid-charging solutions. It is seen that the electrode potential for the hydrogen evolution reaction is more noble on Pt-implanted than on unimplanted surfaces. As a result, the degree of hydrogen coverage, θ, and the permeability of hydrogen should be less for Pt-implanted than for unimplanted iron membranes (19,13,4) in accord with the permeation results in Figures 3 and 5. The above reasoning also applies to the decrease of the steady-state permeation and more positive electrode potential with increasing amount of Fe dissolution which corresponds to increasing Pt content of the surface (Figure 6). The latter is confirmed by the Rutherford backscattering data which show an initial increase in the surface concentration of Pt with dissolution time (Figure 2). A correspondence of the electrochemical and the backscattering data also holds at longer dissolution times. A reversal in the trends of both E_c and i_∞ at 40 seconds in Figure 6 is attributable to a loss of Pt from the surface, in accord with the backscattering profile data (Figure 2). The earlier reversal of the backscattering data in Figure 2 is consistent with the use of a higher concentration of sulfuric acid. That continued dissolution of the membrane eventually leads to Pt loss from the surface is supported by the approach after long times of the i_∞ and E_c values to those for unimplanted Fe membranes at the same value of i_c.

In summary, the mechanism by which implanted Pt reduces hydrogen absorption by iron is related to the different catalytic tendencies of Pt and Fe for the hydrogen evolution reaction. In this case, the hydrogen evolution reaction occurs more easily (lower overvoltage required) on Pt than on Fe sites; thus, the coverage of hydrogen on the mixed Pt-Fe surface is lower and, consequently, so also is the absorption rate (4).

Thus, these results indicate that for ion implantation in iron to be effective for reducing hydrogen absorption, ion implants should have a higher exchange current density for hydrogen evolution than that for the substrate metal. The data also show for implanted Pt that modifications of the implantation profile, which increase the concentration of the implant in the outermost surface layer, increase evolution and decrease absorption of hydrogen.

The data in Table 2 for He- and Fe-implanted iron show that there are no significant differences in the polarization or permeation behavior between unimplanted and implanted iron. Furthermore, the Tafel slopes are also the same. Thus, the implantation process, in itself, does not modify the mechanism of, or the catalytic character of the surface for, the hydrogen evolution reaction. Ashworth, et al. (5), also found that once the air formed oxide is removed, the polarization behavior of unimplanted and argon-implanted iron is nearly the same. A delay in the permeation-kinetics, on the other hand, might have been expected for the implanted membrane since the implantation process, itself, introduces defects to about the depth of the profile. In recent ion beam studies of deuterium-implanted iron, Myers et al. (20), found that the activation energy of a deuterium trap produced by the implantation process is 0.81 eV, that slow release from the traps occurs between 300 and 400K, and that either deuterium or iron ions create the traps. The presence of effective hydrogen traps can, in principle, be indicated by a comparison of the permeation rise times for unimplanted and implanted membranes. That the half-rise times in the present measurements were the same within the experimental error may be attributed to (i) modifications of the nature or density of the traps during the long (~9 mo.) delay between the implantation process and the permeation measurements, (ii) filling of the traps with hydrogen from other sources during the above mentioned delay, and/or (iii) a lack of sensitivity in the measurement.

Some of the data obtained in this work are of the type normally used for evaluation of the mechanism of the hydrogen evolution reaction. It has been shown elsewhere (13,18,19) that if hydrogen evolution occurs via a coupled discharge-recombination mechanism, as is the case for iron, the following relations are obtained at low hydrogen coverages, θ, for rate controlling diffusion through the membrane,

$$i_\infty \alpha i_c^{1/2} \tag{1}$$

$$\frac{\partial \eta}{\partial \ln i_\infty} = \frac{\partial \eta}{\partial \ln \theta} = -\frac{4RT}{F} \tag{2}$$

and

$$\frac{\partial \eta}{\partial \ln i_c} = -\frac{2RT}{F} \tag{3}$$

where η is the overpotential for hydrogen evolution, F the Faraday, R the gas constant and T the temperature. In this investigation it was found that the steady-state permeation current is directly proportional to the square root of the charging current density (Figure 3 and Table 2) for Fe- or He-implanted and unimplanted iron membranes. Furthermore, the Tafel slope (Figure 4) is -122 ± 5 mV and $\partial\eta/\partial\ln i_\infty$ = -255 ± 5 mV (Figure 5) in reasonably good agreement with Eqs. (3) and (2), respectively. At higher cathodic overpotentials in 0.1N NaOH, corresponding to potentials more negative than -1.0 V (SHE), there appears to be a change in mechanism for the unimplanted and Fe- or He-implanted membranes to slow discharge-fast electrochemical desorption, as indicated by an increase in $\partial\eta/\partial\ln i_\infty$, Figure 5 (17,19).

For Pt-implanted Fe, the Tafel slope again is -122 ± 5 mV and $\partial\eta\ \partial\ln i_\infty$ = -255 ± 5 mV and the steady-state permeation varies linearly through the origin with the square root of the charging current density. Thus, it is concluded that the mechanism for Pt-implanted Fe is also coupled discharge-chemical

desorption in both the 0.1N NaOH and 0.1N H_2SO_4 solutions within the overpotential range studied. The Tafel slope reported in the literature for hydrogen evolution on Pt surfaces is in two different ranges, either -110 to -130 mV in NaOH solutions (21-24) or about -30 mV in H_2SO_4 solutions (23) for ultra clean systems. Tafel slopes greater than -30 mV in H_2SO_4 have, however, been observed in the presence of impurities (25).

The Rutherford backscattering data also provide insight into the mechanism of selective dissolution of iron from the Fe-Pt surface layer. During the first 20 seconds of immersion in acid the Pt-implanted Fe membrane lost 10^2 nm (or more) of iron from the surface, corresponding to an estimated average iron dissolution rate of 10^{-2} A cm^{-2}. After this 20-second immersion the originally polished (6μm diamond) surface appeared rough, had completely lost its reflective properties and was gray in color. This relatively large amount of dissolution, compared to the depth of the implanted Pt profile (~40 nm), needs to be reconciled with the fact that the Pt profile shows a similar amount of Pt and distribution over about 40 nm after, as before, iron dissolution, Figure 2. Discounting uncertainties with regard to the amount of iron removed and to the effect of surface roughening during dissolution, an explanation of the backscattering results requires the motion of Pt into the iron ahead of the receding surface. A driving force for diffusion of Pt back into the iron exists in the activity gradient developed by accumulation of Pt on the surface. Although one may question whether the kinetics are adequate, such a process has already been considered and shown to operate in some alloy systems (26-30). The present situation differs slightly from one of the available models of preferential dissolution. In this model (29,31), the interdiffusion distance obtains a constant value by virtue of a finite dissolution rate of the more noble metal. In the case of ion implantation, it can readily be shown that the interdiffusion distance obtains a constant value so long as no platinum is lost from the surface.

In the present work the diffusion distance is on the order of 40 nm based on the depth of the Pt profile after the 20-second immersion. Thus, it would appear that the so-called volume diffusion mechanism of preferential dissolution of one component from an alloy operates during initial selective dissolution of iron from the Pt-implanted iron surface. Similar Rutherford backscattering profiles before and after immersion in acid have been reported for Pd-implanted Ti samples (11).

The eventual loss of Pt from the surface region may be attributed to accumulation and detachment of platinum as small particles. Such a process is known to occur for low percentages ($\lesssim$1%) of the noble metal in solid solution (28), and is in accord with industrial experience, especially during electrolytic refining of copper containing small amounts of Au.

CONCLUSIONS

Ion implantation can be used to reduce hydrogen entry into iron. This was shown using the (model) system of Pt implanted into Fe. Pt is known to greatly reduce hydrogen entry into iron via a catalytic effect on the hydrogen evolution reaction when the Pt is present on the surface (4). The effectiveness of implanted Pt was greatly increased by controlled selective dissolution of iron which increased the surface concentration of Pt. There are no significant differences in the permeation behavior of unimplanted and He- or Fe-implanted Fe specimens.

The experimentally observed Tafel slope, the permeation-charging potential relationship, and the permeation-charging current relationship indicate a coupled discharge-recombination mechanism of hydrogen evolution on Fe-, He- or Pt-implanted Fe surfaces in 0.1N NaOH or 0.1N H_2SO_4 charging solutions.

The Rutherford backscattering profiles taken before and after selective dissolution of iron from the Pt-implanted Fe samples show that the as-implanted

Pt distribution (depth ≃ 40 nm) is maintained during removal of even greater equivalent thicknesses of iron. These results are consistent with the volume diffusion mechanism of preferential dissolution of a component from solid solution (26).

ACKNOWLEDGEMENT

This work was partially supported by the Metallurgy Branch of the Office of Naval Research under Contract N000-14-75-C-0264.

REFERENCES

1. M. A. Figelman and A. V. Shreider, J. Appl. Chem. (USSR) 31, 1175 (1958).
2. T. Matsushima and H. H. Uhlig, J. Electrochem. Soc. 113, 555 (1966).
3. H. P. Tadrif and H. Marquis, Can. Meta. Quart. 1, 153 (1962).
4. S. S. Chatterjee, B. G. Ateya and H. W. Pickering, Met. Trans. 9A, 389-95 (1978).
5. V. Ashworth, W. A. Grant, R. P. M. Procter and T. C. Wellington, Corr. Sci. 16, 393 (1976).
6. V. Ashworth, D. Baxter, W. A. Grant and R. P. M. Procter, Corr. Sci. 16, 775 (1976).
7. V. Ashworth, W. A. Grant, R. P. M. Procter and E. J. Wright, Corr. Sci. 18, 681 (1978).
8. H. W. Pickering and P. J. Byrne, J. Electrochem. Soc. 120, 608 (1973).
9. R. W. Powers, Electrochem. Technol. 2, 163 (1969).
10. M. A. V. Devanathan and Z. Stachurski, Proc. Roy. Soc. A270, 90 (1962).
11. G. K. Hubler and E. McCafferty, to be published in Corrosion Science.
12. J. K. Hirronen and G. K. Hubler, Ion Beam Surface Layer Analysis, ed. O. Meyer, G. Linker and F. Käppeler, Plenum, New York,(1976), Vol. 1, p. 457.
13. J. McBreen, L. Nanis and W. Beck, J. Electrochem. Soc. 113, 1218 (1966).
14. J. O'M. Bockris, Proceedings of International Conference on Stress Corrosion Cracking and Hydrogen Embrittlement of Iron Base Alloys, Firminy, France, p. 286, June 1973.
15. T. R. Radhakrishan and L. L. Shreir, Electrochimica Acta 12, 889 (1967).
16. O. D. Gonzalez, Trans. Met. Soc. AIME 239, 229 (1967).
17. J. O'M. Bockris, J. McBreen and L. Nanis, J. Electrochem. Soc. 112, 1025 (1965).
18. J. McBreen and M. A. Genshaw, Proceedings of the International Conference on Fundamental Aspects of Stress Corrosion Cracking, R. W. Staehle, A. J. Forty and D. van Rooyan, Eds., p. 51, NACE, 1969.
19. M. A. V. Devanathan and Z. Stachurski, J. Electrochem. Soc. 111, 619 (1964).
20. S. M. Myers, S. T. Picraux and R. E. Stoltz, to be published in J. of Appl. Phys.
21. S. Schuldiner, J. Electrochem. Soc. 107, 426 (1954).
22. I. A. Ammar and S. Darwish, J. Phys. Chem. 63, 983 (1959).
23. J. O'M. Bockris and S. Srinivasan, Electrochimica Acta 9, 31 (1964).

24. C. M. Shepherd and S. Schuldiner, J. Electrochem. Soc. 115, 1124 (1968).

25. J. O'M. Bockris, I. A. Ammar and A. K. M. S. Huq, J. Phys. Chem. 61, 879 (1957).

26. H. W. Pickering and C. Wagner, J. Electrochem. Soc. 114, 698 (1967).

27. H. W. Pickering, J. Electrochem. Soc. 115, 143 (1968).

28. H. W. Pickering, J. Electrochem. Soc. 117, 8 (1970).

29. J. E. Holliday and H. W. Pickering, J. Electrochem. Soc. 120, 470 (1973).

30. H. W. Pickering, "Darken Conference: Physical Chemistry in Metallurgy", R. M. Fisher, R. A. Oriani and E. T. Turkdogan, Eds., U. S. Steel Corporation, Pittsburgh, Pa. (1976), pp. 353-73.

31. H. W. Pickering, J. Vac. Sci. Technol. 13, 618 (1976).

TABLE 1

Energies and fluences of implanted ions in iron membranes

Ion	Energy, KeV	Fluence, ions/cm^2
Fe	150	1×10^{17}
Pt	100	1.5×10^{16}
He	25	1.6×10^{17}

TABLE 2

Variation of the steady state hydrogen permeation flux and of the electrode potential at the charging side with the charging current density for an unimplanted Fe membrane and for an identical membrane implanted with He or Fe. Charging solution was 0.1N NaOH.

charging current density, mA/cm^2	steady state permeation rate and electrode potential of the charging side					
	unimplanted iron		He-implanted iron		Fe-implanted iron	
	$i_\infty, \mu A/cm^2$	$-E_C$, v(SHE)	$i_\infty, \mu A/cm^2$	$-E_C$, v(SHE)	$i_\infty, \mu A/cm^2$	$-E_C$, v(SHE)
0.1	1.77	1.005	1.78	1.005	1.65	1.00
0.08	1.50	0.990	1.46	0.989	1.45	0.990
0.06	1.32	0.975	1.27	0.974	1.27	0.975
0.04	1.02	0.950	1.02	0.950	1.01	0.950
0.02	0.70	0.910	0.74	0.910	0.67	0.910

TABLE 3

Variation of the steady state hydrogen permeation flux and of the electrode potential of the charging side with the charging current density for an unimplanted Fe membrane and for an identical membrane implanted with Pt. Charging solution was 0.1N H_2SO_4.

charging current density mA/cm^2	steady state permeation rate and electrode potential of the charging side			
	unimplanted iron		Pt-implanted iron	
	i_∞ $\mu A/cm^2$	-E, v(SHE)	i_∞ $\mu A/cm^2$	-E, v(SHE)
1.0	22.0	0.425	16.2	0.407
0.8	20.0	0.415	14.5	0.395
0.6	17.5	0.400	12.5	0.380
0.4	14.2	0.380	10.5	0.360
0.2	10.2	0.345	7.5	0.325
0.1	7.3	0.310	5.5	0.290

FIGURE CAPTIONS

Figure 1. Hydrogen permeation transients for He-implanted Fe and Pt-implanted Fe membranes. i_c = 0.1 mA cm^{-2} in 0.1N NaOH.

Figure 2. Profiles of implanted Pt in Fe as a function of time of immersion of the implanted sample in 1M H_2SO_4 at room temperature. Depth of resolution is 4 nm (40Å).

Figure 3. Steady state permeation rate i_∞ as a function of the square root of the charging current density i_c for an unimplanted Fe membrane and a Pt-implanted and acid treated Fe membrane. Charging solution was 0.1N NaOH.

Figure 4. The polarization curve in the Tafel region for hydrogen evolution in 0.1N NaOH on an unimplanted iron (o) and a Pt-implanted Fe membrane following a 20-second immersion in 1M H_2SO_4 (□).

Figure 5. Steady state permeation rate i_∞ as a function of the potential of the charging surface of the membrane, E_c. Charging solution was 0.1N NaOH.

Figure 6. Steady state permeation rate (□) and charging potential (o) as a function of additional immersion periods in 0.1N H_2SO_4 beyond the initial 20-second immersion in 1M H_2SO_4 of the Pt-implanted surface. Charging current was 0.6 mA cm^{-2} in 0.1N H_2SO_4.

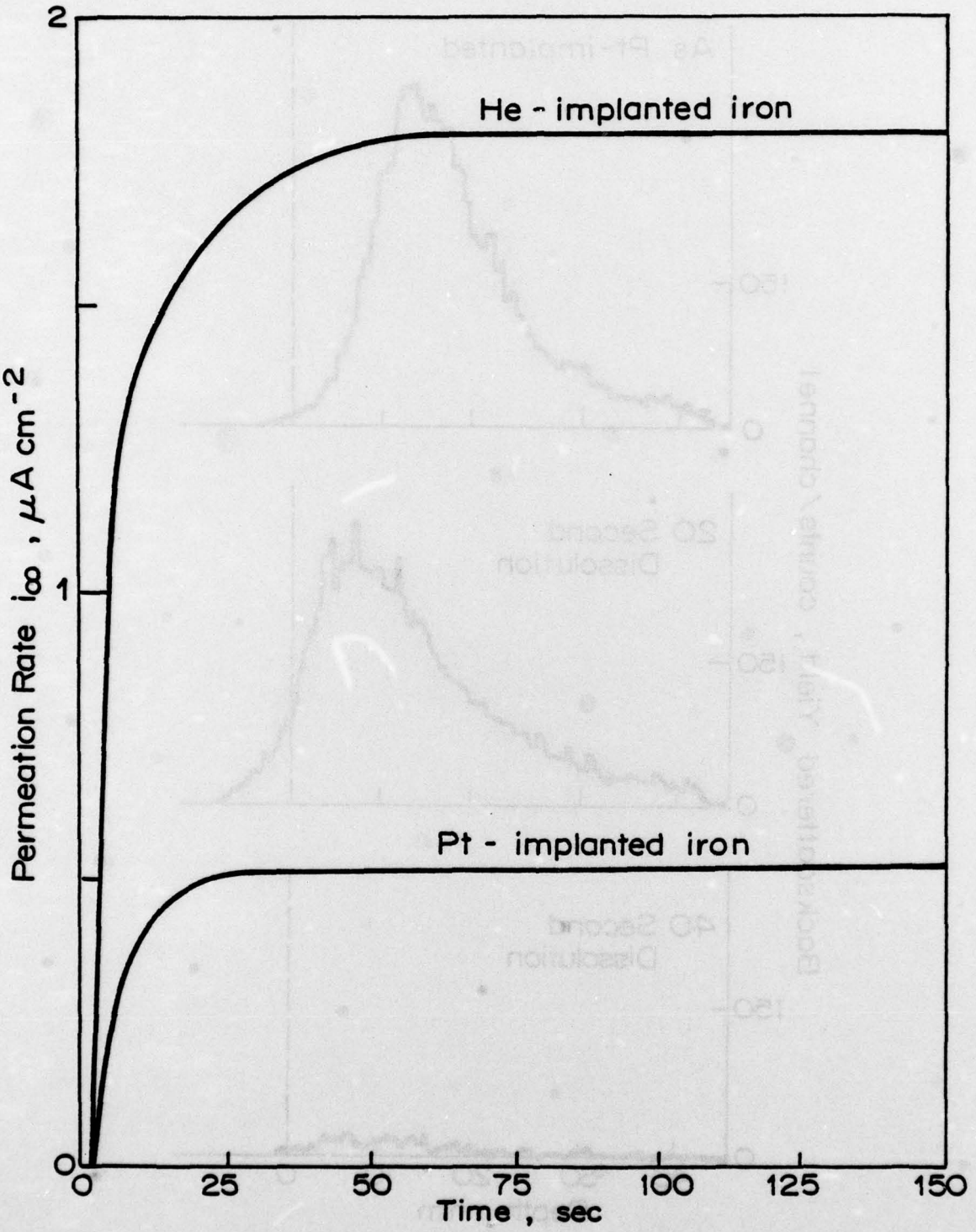

Figure 1. Hydrogen permeation transients for He-implanted Fe and Pt-implanted Fe membranes. i_c = 0.1 mA cm^{-2} in 0.1NaOH.

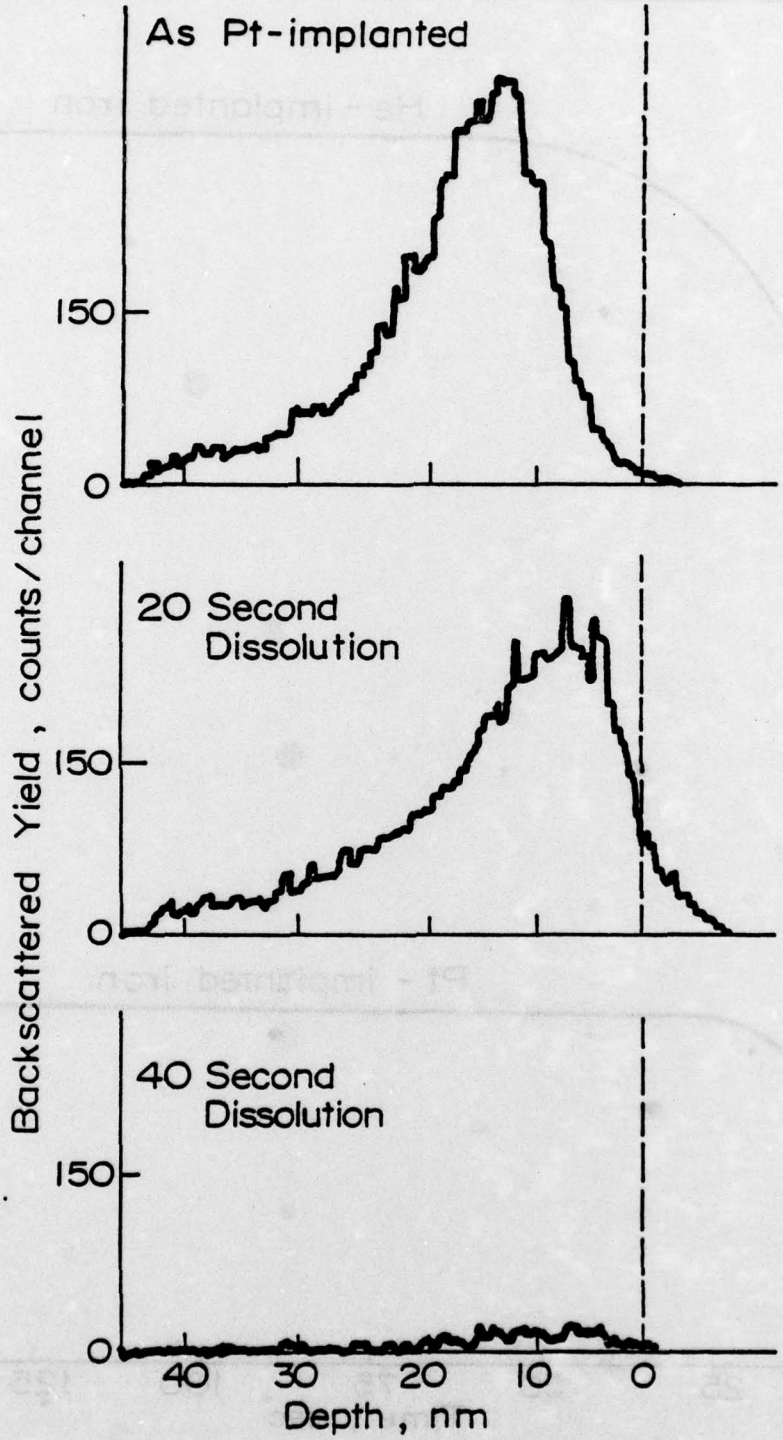

Figure 2. Profiles of implanted Pt in Fe as a function of time of immersion of the implanted sample in 1M H_2SO_4 at room temperature. Depth of resolution is 4 nm (40Å).

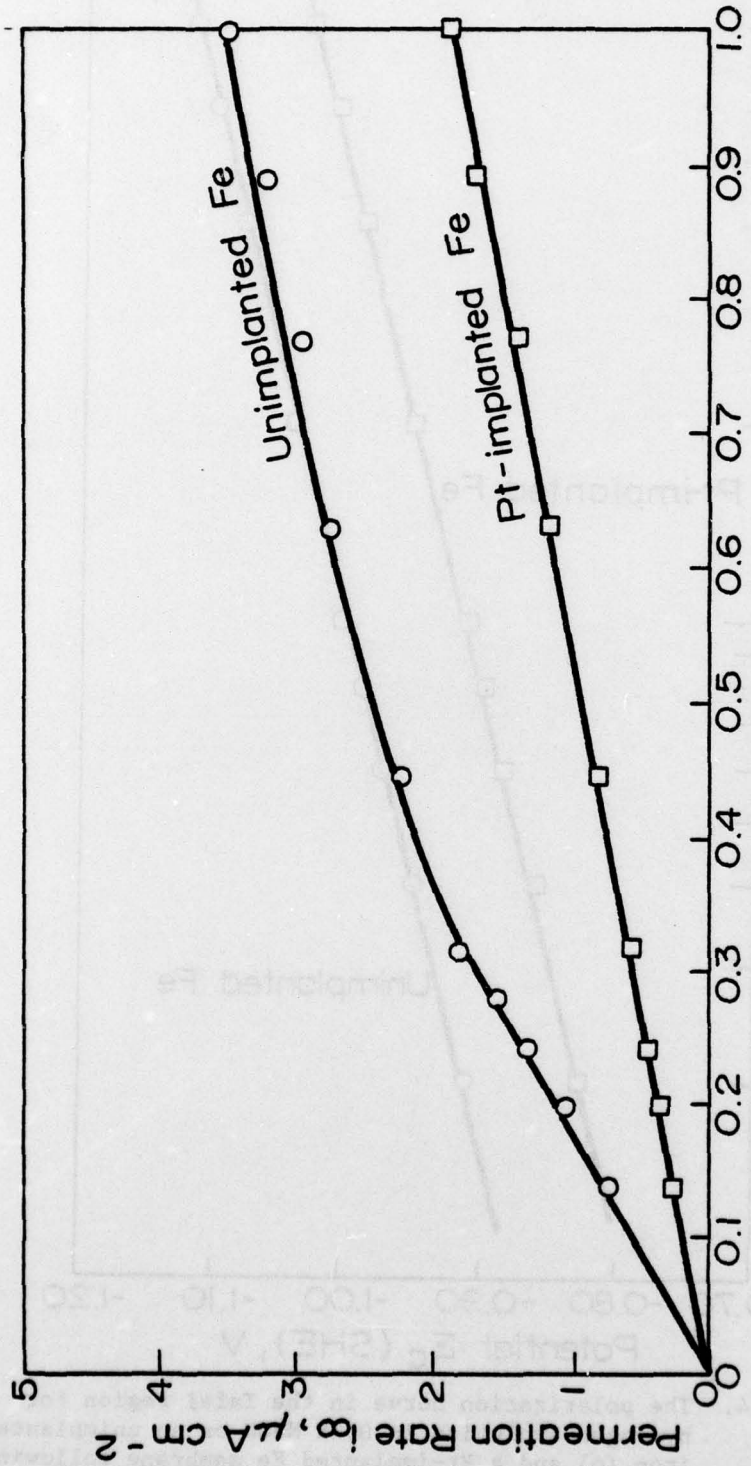

Figure 3. Steady state permeation rate i_∞ as a function of the square root of the charging current density i_c for an unimplanted Fe membrane and a Pt-implanted and acid treated Fe membrane. Charging solution was 0.1N NaOH.

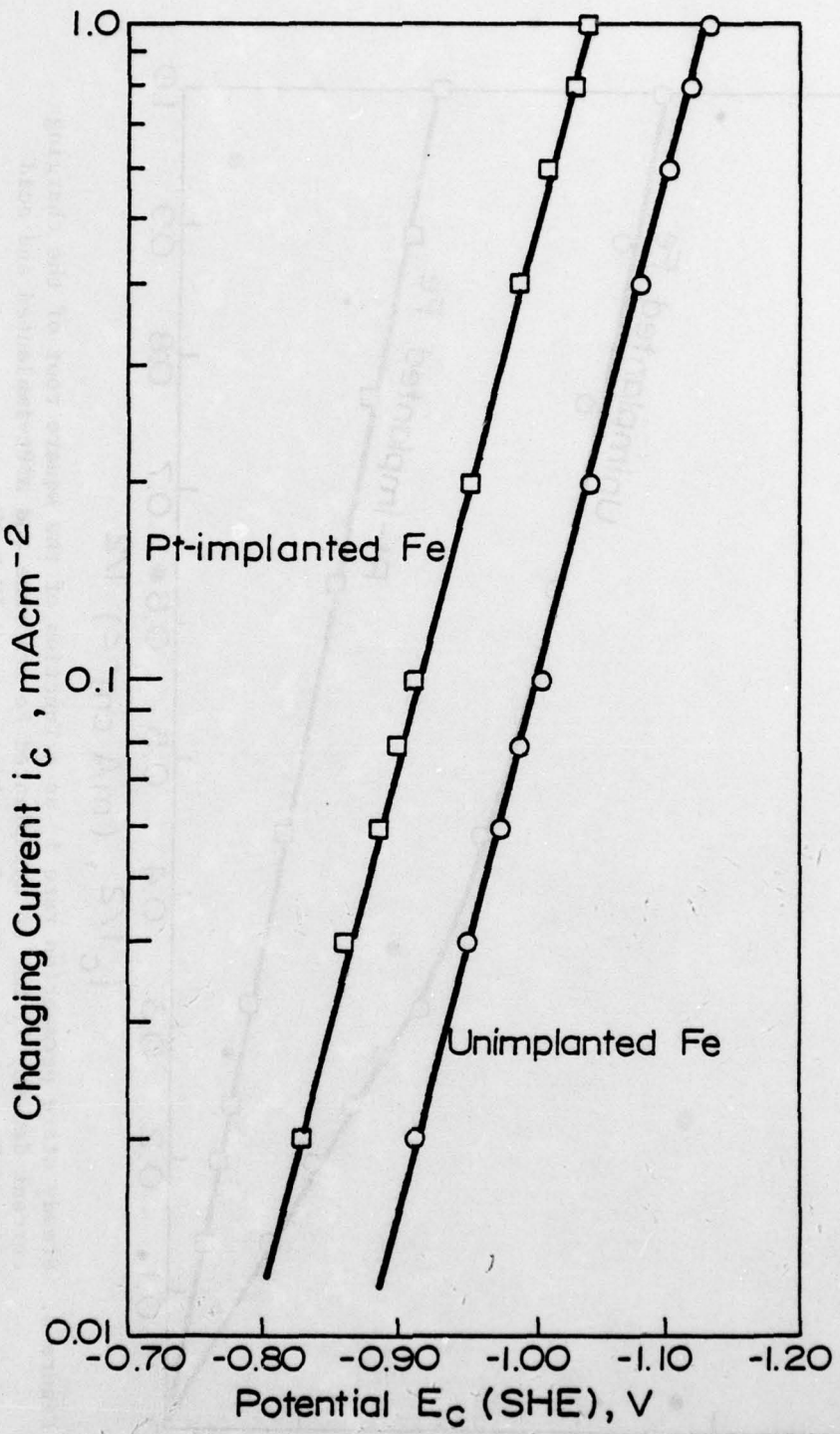

Figure 4. The polarization curve in the Tafel region for hydrogen evolution in 0.1N NaOH on an unimplanted iron (o) and a Pt-implanted Fe membrane following a 20-second immersion in 1M H_2SO_4 (□).

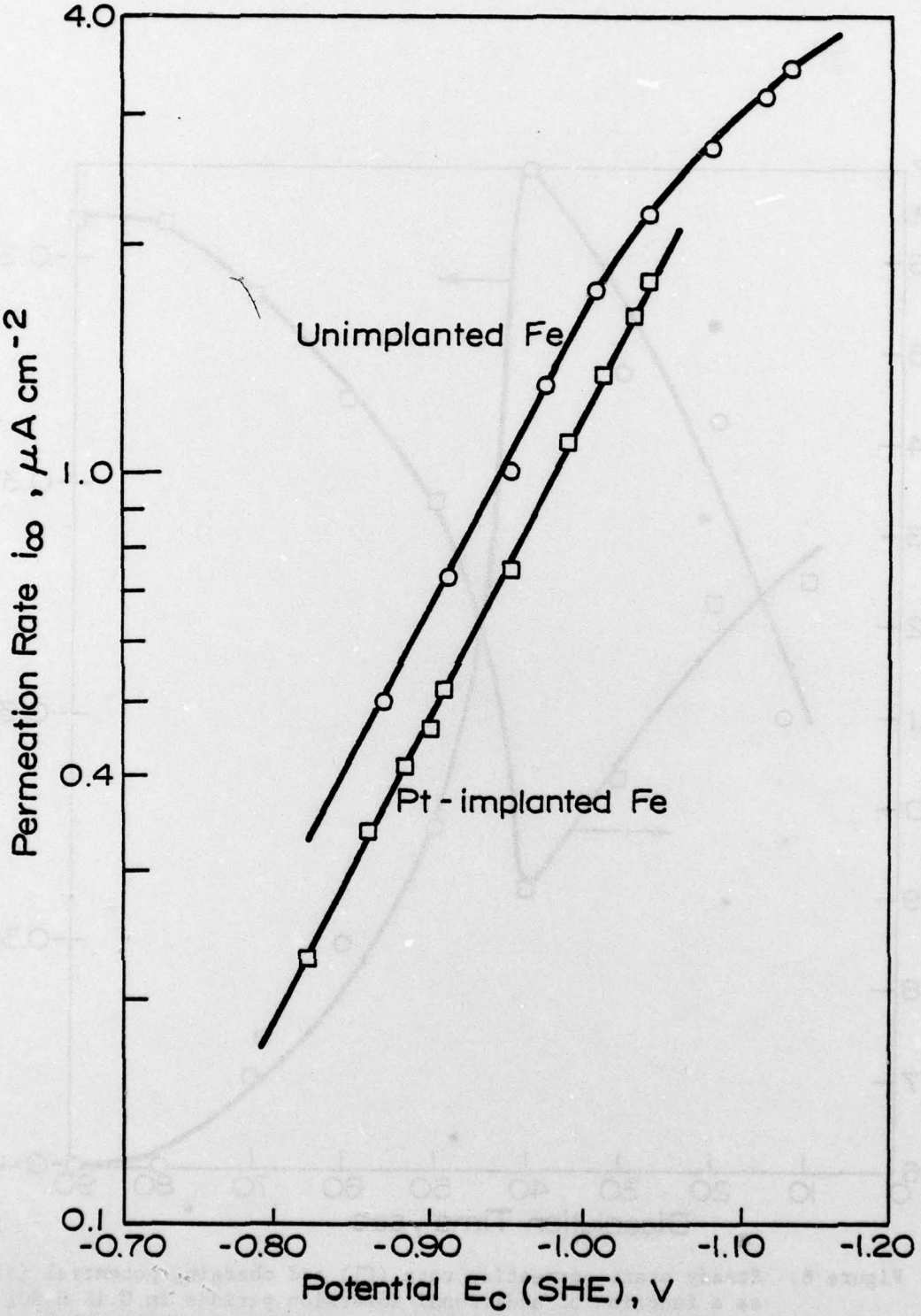

Figure 5. Steady state permeation rate i_∞ as a function of the potential of the charging surface of the membrane, E_c. Charging solution was 0.1N NaOH.

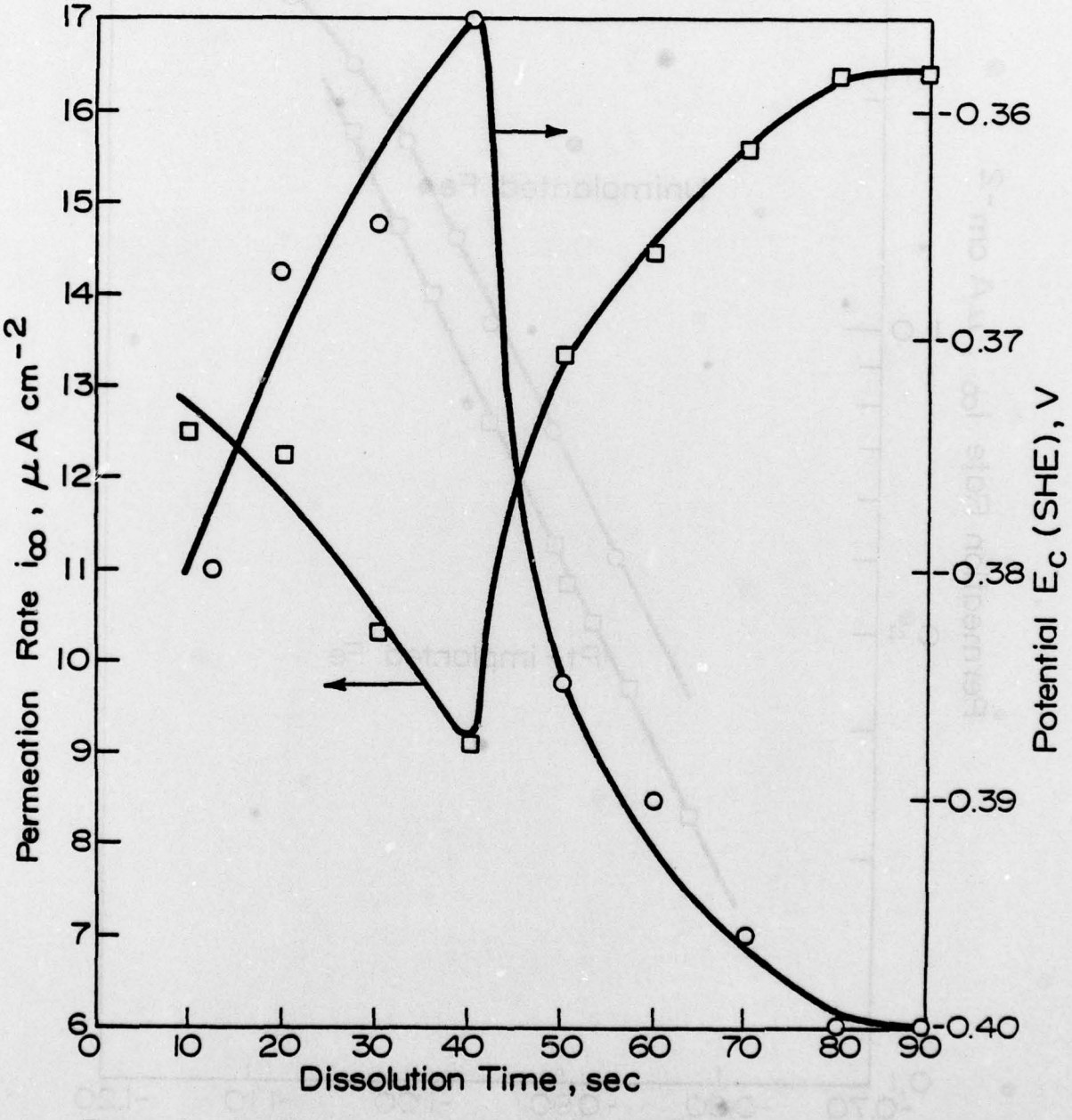

Figure 6. Steady state permeation rate (□) and charging potential (o) as a function of additional immersion periods in 0.1N H_2SO_4 beyond the initial 20-second immersion in 1M H_2SO_4 of the Pt-implanted surface. Charging current was 0.6 mA cm^{-2} in 0.1N H_2SO_4.